Asynchronous Periodic Distributed Event-Triggered Voltage and Frequency Control of Microgrids

Keywan Mohammadi, Elnaz Azizi, *Graduate Student Member, IEEE*, Jeewon Choi, *Student Member, IEEE*, Mohammad-Taghi Hamidi-Beheshti, *Member, IEEE*, Ali Bidram, *Senior Member, IEEE*, and Sadegh Bolouki, *Member, IEEE*

***Abstract*—In this paper, we introduce a distributed secondary voltage and frequency control scheme for an islanded ac microgrid under event-triggered communication. An integral type event-triggered mechanism is proposed by which each distributed generator (DG) periodically checks its triggering condition and determines whether to update its control inputs and broadcast its states to neighboring DGs. In contrast to existing event-triggered strategies on secondary control of microgrids, the proposed event-triggered mechanism is able to handle the consensus problem in case of asynchronous communication. Under the proposed sampled-data based event-triggered mechanism, DGs do not need to be synchronized to a common clock and each individual DG checks its triggering condition periodically, relying on its own clock. Furthermore, the proposed method efficiently reduces communication rate. We provide sufficient conditions under which microgrid's frequency and a critical bus voltage asymptotically converge to the nominal frequency and voltage, respectively. Finally, effectiveness of our proposed method is verified by testing different scenarios on an islanded ac microgrid benchmark in the MATLAB/Simulink environment as well as a hardware-in-the-loop (HIL) platform, where the physical system is modeled in the Opal-RT and the cyber system is realized in Raspberry Pis.**

***Index Terms*—Asynchronous event-triggered control, distributed secondary control, islanded microgrids, multi-agent systems, voltage and frequency restoration.**

I. Introduction

Emerging distributed energy resources have shaped a new structure in power distribution networks, paving the way for creation of the microgrid concept [1]. In normal operation, microgrids are connected to the main grid and their voltage and frequency are imposed by the upstream grid. A microgrid can get disconnected from the main grid and go to the autonomous mode. Despite the advantages of microgrids in enhancing the power system's flexibility, they present some technical challenges such as control and power management issues. Hence, in microgrids, a hierarchical control scheme is tasked to ensure reliable performance in the face of probable challenges [2].

Decentralized primary controller, which is located at the innermost layer of the hierarchical structure, deals with fast dynamics and stability of the microgrid system [3], [4]. However, the primary control level causes deviations of voltage and frequency from their nominal rating. Therefore, to compensate the steady-state deviations, an outer control layer, namely secondary controller, can be applied. Restoring frequency and voltage magnitudes caused by the primary controller is the main objective of the secondary control level.

Early research on the secondary control of microgrids mitigated steady-state deviations of voltage and frequency in a centralized manner [3]–[5]. However, due to the heavy communicational burden on the central controller and high sensitivity of the network to centralized architectures may reduce the system's reliability. Therefore, distributed cooperative control strategies with sparse and robust communication networks, became appropriate alternatives for the secondary controller design [6].

On the other hand, distributed cooperation and coordination within networked systems have become the focal point of research in a wide variety of scientific and engineering problems [7]–[9]. Considering the problem of frequency and voltage synchronization in microgrids as a leader-follow consensus problem, the secondary control design can be conducted based upon distributed coordination theory in multi-agent systems. In much of the research in this field, considering continuous time communication between DGs as an assumption is evident. However, discrete sample-data interaction is more realistic for data exchange in communication networks. Furthermore, in practice, frequently gathering information and updating control actions exhaust communication and computational capabilities of DGs' digital tools. This has led to the emergence of event-triggered control strategies as sound alternatives to sampled-data techniques [10], [11].

A. Motivation

Almost all the recent efforts in event-triggered secondary control of microgrid systems have been done under the assumption of DGs' capability of continuously or periodically but synchronously measuring their desired states and evaluating the triggering condition during the process. Existing synchronous periodic event-triggered techniques need a globally synchronized clock to synchronize the measurments and communications, according to which all DGs evaluate their event conditions, update their control signals, and broadcast their states to other DGs at precisely same times. However, the GPS clocks may not be readily available on all DGs.

K. Mohammadi, E. Azizi, M. Beheshti, and S. Bolouki are with Department of Electrical and Computer Engineering, Tarbiat Modares University, Tehran, Iran. e-mail:(keywan.mohammadi@modares.ac.ir, e.azizi@modares.ac.ir, mbehesht@modares.ac.ir, bolouki@modares.ac.ir)

J. Choi and A. Bidram are with Department of Electrical and Computer Engineering, The University of New Mexico, Albuquerque, New Mexico. email:(chatchi923@unm.edu, bidram@unm.edu). J. Choi and A. Bidram are supported by the National Science Foundation EPSCoR Program under Award OIA-1757207.

Moreover, even assuming that DGs are equipped with GPS clock based time synchronization system, they are still exposed to GPS time spoofing attacks which cause asynchronous measurements. The GPS time spoofing attacks deteriorate the performance of control system and may lead to detrimental consequences like blackouts [12]. As a result, this paper proposes a novel distributed event-triggered secondary control in order to answer these drawbacks and difficulties and generalize the previous results to the best of our knowledge.

B. Related Work

The very first attempts to design secondary controller utilizing distributed cooperative control theory were [6] and [13]. In these articles, the nonlinear and heterogeneous dynamics of the DGs are transformed to the linearized dynamics using feedback linearization method. Consequently, the voltage and frequency restoration problem resembles a linear distributed tracking problem which has been widely studied in the multi-agent systems literature. In [14], authors introduce a finite-time framework for the distributed secondary controller, by which the frequency regulation and active power sharing are well achieved while a decoupled design for voltage regulation and reactive power sharing at different time scales with the frequency controller is enabled. Considering noisy measurements, a distributed noise-resilient secondary control is proposed in [15], in which a mean-square average-consensus protocol has been employed to regulate voltage and frequency in case of corrupted communication channels. Time delay effects on the secondary control layer is thoroughly addressed in reference [16], showing that the model predictive controller has more robustness in case of time delays. In [17], the model based distributed controllers are designed firstly and then adaptive neural networks are utilized to approximate the uncertain/unknown dynamics of the microgrid system.

Event-triggered techniques have been investigated in distributed secondary control of microgrid systems in [18]–[21]. In [18], a distributed secondary active power sharing and frequency control, based on a sample-based event-triggered communication strategy, is proposed that effectively reduces the communication complexity. In [19], an event-triggered communication-based consensus control for dc microgids is proposed, in which stability of the micgrogrid system during different stressful conditions is guaranteed. Authors in [20] utilized an event-triggered mechanism for active and reactive power sharing of microgrids. Considering uncertainties a distributed H_∞ consensus approach with an event-triggered communication scheme is presented in [21].

C. Contributions

To the best of authors' knowledge, no research has been dedicated to the asynchronous event-triggered secondary control problem of microgrid systems yet. In our proposed method, each DG is equipped with its own clock and may have different event-checking instants from the rest of the system. Cyber network problems under asynchronous communication are clearly more complicated than those under synchronous communication, as the latter set of problems can be viewed as special cases of the former. In order to fill this gap, this paper investigates the cooperative secondary control problem of ac microgrid systems based on asynchronous periodic event-triggered strategy, bringing model one step closer to reality. This paper has the following salient contributions that, to the best of our knowledge have not been exploited yet:

- A distributed secondary voltage and frequency scheme using an event-triggered mechanism is proposed. It is demonstrated that the proposed mechanism is able to achieve a nearly identical voltage and frequency regulation while reducing the rate of communication.
- Compared with existing event-triggered mechanisms on secondary control of microgrids, this paper is the first to propose an event-checking mechanism which is capable of coping with the asynchronous behavior of communication system. From a practical perspective, unlike traditional synchronized event-triggered mechanisms, our model setup does not require DGs to be coordinated to a global synchronized clock. Therefore, implementation of our proposed mechanism is more practical than existing GPS clock based mechanisms.
- The proposed distributed event-triggered control scheme is validated on an experimental testbed implemented on a hardware-in-the-loop (HIL) platform. The HIL results demonstrate the effectiveness of the proposed method through different test scenarios.

The remainder of this paper is organized as follows. Section II presents the preliminaries of graph theory, while Section III provides the dynamical modeling of an autonomous microgrid. The proposed secondary frequency and voltage control schemes are presented in section IV. In Section V, the effectiveness of the proposed secondary control method is validated on a microgrid test system using MATLAB/Simulink software environment and HIL platform. Section VI discusses obtained results and main achievements of the paper. The paper is summarized in section VII , where future directions of this research are stated. Finally, the proof of our main result is given in the Appendix.

II. Preliminaries on Graph Theory

In this work, we consider a network of DGs whose communication topology is represented by a weighted, directed , simple graph $\mathcal{G} = (V, E, A)$, in which $V = \{v_1, v_2, \ldots, v_n\}$ is the set of nodes, each representing a DG, $E \subset V \times V$ represents the edge sets, each representing a directed communication channel from a DG to another, and $A = [a_{ij}] \in R^{n\times n}$ is the generalized adjacency matrix formed by edge weights of the graph that are all assumed non-negative. Concretely, an edge from DG i to DG j exists if there is a communication channel from DG i to DG j, i.e., DG i is able to send data to DG j. We notice that this channel of communication can be as well inferred from the value of a_{ij}. More precisely, DG i is able to send data to DG j if and only if $a_{ij} > 0$. The graph Laplacian matrix of $\mathcal{G}$ is defined as $L = [l_{ij}] \in \mathbb{R}^{(n\times n)}$, in which $l_{ii} = \sum_{j\neq i} a_{ij}$ and $l_{ij} = -a_{ij}$. A directed path from v_i to v_j is a sequence of edges, expressed as $\{(v_i, v_k), (v_k, v_l), ..., (v_m, v_j)\}$. A directed graph is called

This article has been accepted for publication in a future issue of this journal, but has not been fully edited. Content may change prior to final publication. Citation information: DOI 10.1109/TPWRS.2021.3059158, IEEE Transactions on Power Systems

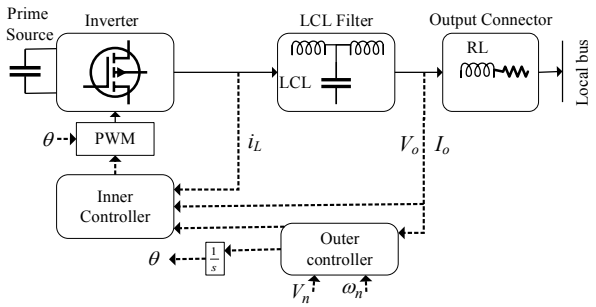

Fig. 1: Block diagram of an inverter-based DG.

strongly connected if there exists a directed path from any node to any other node [22].

Lemma 1. [23] *If $\mathcal{G}$ is a strongly connected directed graph with Laplacian matrix L, there exists a vector $w = [w_1, w_2, \ldots, w_n]$ with all positive elements such that $wL = 0$. Furthermore, defining $W = diag(w_1, w_2, \ldots, w_n)$, the matrix $WL + L^T W$ is semi definite.*

III. Dynamical Modeling of an Autonomous Microgrid

A microgrid is a complex dynamical system consisting of physical layers, control layers, and cyber infrastructures. An inverter-based DG as the main building block of the microgrid system is depicted in Fig. 1. The large signal dynamical model of each DG is represented on its own direct and quadrature (d-q) reference frame. For constructing the model of the entire system, the reference frame of one DG is assigned as the common frame with the rotating frequency of $\omega_{\rm com}$. The dynamics of other DGs must then be translated to this common one, i.e., loads and lines dynamics are represented on the common frame. Details on transformation equations are provided in [24].

Compensating voltage and frequency deviations can be defined as a steady-state error elimination problem. Thus, for the secondary controller design, neglecting fast dynamics of inner loops due to their poor effects on the steady-state performance of the microgrid system could be permissible [6], [25]. Accordingly, they are in this case removed from the modeling equations [6]. Then, the algebraic equations of the droop controller are written as [6]

$$\begin{cases} \omega_i = \omega_{ni} - m_{Pi} P_i \\ v^*_{odi} = V_{ni} - n_{Qi} Q_i \\ v^*_{oqi} = 0 \end{cases}, \tag{1}$$

where ω_{ni} and V_{ni} are respectively the nominal setpoint of rotating frequency and the output voltage provided by the secondary controller. Internal control loops voltage references are v^*_{odi} and v^*_{oqi}. The operating frequency of $i^{\rm th}$ inverter bridge is ω_i. The LC filter and output connector differential equations are expressed in the following ($v_{id} = v^*_{od}$) [24]:

$$\begin{cases} \dot{i}_{ldi} = \frac{-r_{fi}}{L_{fi}} i_{ldi} + \omega_i i_{lqi} + \frac{1}{L_{fi}} v_{idi} - \frac{1}{L_{fi}} v_{odi} \\ \dot{i}_{lqi} = \frac{-r_{fi}}{L_{fi}} i_{lqi} - \omega_i i_{ldi} + \frac{1}{L_{fi}} v_{iqi} - \frac{1}{L_{fi}} v_{oqi} \\ \dot{v}_{odi} = \omega_i v_{oqi} + \frac{1}{C_{fi}} i_{ldi} - \frac{1}{C_{fi}} i_{odi} \\ \dot{v}_{oqi} = -\omega_i v_{odi} + \frac{1}{C_{fi}} i_{lqi} - \frac{1}{C_{fi}} i_{oqi} \\ \dot{i}_{odi} = \frac{-r_{ci}}{L_{ci}} i_{odi} + \omega_i i_{oqi} + \frac{1}{L_{ci}} v_{odi} - \frac{1}{L_{ci}} v_{bdi} \\ \dot{i}_{oqi} = \frac{-r_{ci}}{L_{ci}} i_{oqi} - \omega_i i_{odi} + \frac{1}{L_{ci}} v_{oqi} - \frac{1}{L_{ci}} v_{bqi} \end{cases}. \tag{2}$$

Equations (1) and (2) can be written in a multi-input multi-output (MIMO) nonlinear compact form as

$$\begin{cases} \dot{x}_i = f_i(x_i) + g_{i1}(x_i) u_{i1} + g_{i2}(x_i) u_{i2} + k_i(x_i) D_i \\ y_i = h_i(x_i) \end{cases}, \tag{3}$$

where $x_i = [i_{ldi}, i_{lqi}, v_{odi}, v_{oqi}, i_{odi}, i_{oqi}]^T$ consists of the direct and quadratic components of i_{li}, v_{oi} and i_{oi}, $u_i = [u_{i1}, u_{i2}]^T = [\omega_{ni}, V_{ni}]^T$, $D_i = [v_{bdi}, v_{bqi}]^T$ are control and disturbance inputs, respectively, and $y_i = [y_{i1}, y_{i2}]^T = [v_{odi}, \omega_i]^T$ is formed by the output voltage and frequency. Since the magnitude of the DG output voltage is

$$v_{o,{\rm mag}i} = \sqrt{{v_{odi}}^2 + {v_{oqi}}^2}. \tag{4}$$

The regulation of the output voltage magnitude, $v_{o,{\rm mag}i}$, is the same as regulation the direct term of output voltages v_{odi}.

IV. Asynchronous Periodic Event-Triggered Secondary Voltage and Frequency Control

We consider an islanded ac microgrid with N DGs, each of which contains a primary source, voltage source inverter (VSI), an LC filter, and an output connector. A basic control framework of the primary control layer is shown in Fig. 1. In what follows, first the problem statement is presented, and then, the proposed asynchronous periodic event-triggered distributed secondary voltage and frequency controllers are developed.

A. Problem Statement

In this paper, the objective is to regulate the operating frequency and output voltage magnitude of DGs in an islanded ac microgrid based on distributed cooperation control of multi-agent systems. This controller selects proper control inputs ω_{ni} and V_{ni} in (1) to restore the operating frequency and output voltage magnitude of DGs, ω_i and $v_{o,{\rm mag}i}$, to their reference values, $\omega_{\rm ref}$ and $v_{\rm ref}$. We herein assume that the communication framework among DGs is described by a strongly connected directed graph. Recalling the frequency and voltage droop characteristic in (1) and considering (4), one can establish a relation between DG's operating frequency ω_i and output voltage magnitude $v_{o,{\rm mag}i}$ and control inputs, ω_{ni} and V_{ni} as

$$\begin{cases} \omega_i = \omega_{ni} - m_{Pi} P_i \\ v_{o,{\rm mag}i} = V_{ni} - n_{Q_i} Q_i \end{cases}. \tag{5}$$

This article has been accepted for publication in a future issue of this journal, but has not been fully edited. Content may change prior to final publication. Citation information: DOI 10.1109/TPWRS.2021.3059158, IEEE Transactions on Power Systems

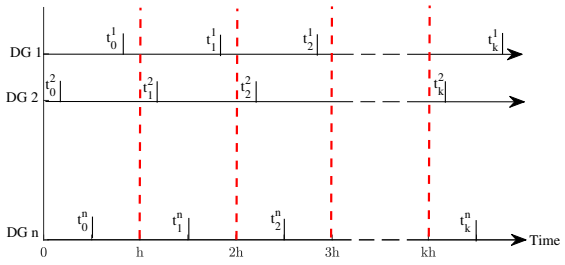

Fig. 2: Event-checking time instants of the DGs.

Differentiating both sides of (5) and defining auxiliary control inputs $u_{\omega i}$ and u_{vi}, one has

$$\begin{cases} \dot{\omega}_i = \dot{\omega}_{ni} - m_{Pi}\dot{P}_i = u_{\omega_i} \\ \dot{v}_{o,\mathrm{mag}i} = \dot{V}_{ni} - n_{Qi}\dot{Q}_i = u_{v_i} \end{cases}, \tag{6}$$

where u_{ω_i} and $u_{v_i} \in \mathbb{R}$.

In this work, we consider the problem of asynchronous behavior of the communication network in microgrid systems. It is assumed that the local secondary frequency and voltage controllers of each DG, described by (6), sample their desired states at fixed period times, relying on their own clocks. This is an arguably expected behavior for real-world multi-agent systems like microgrids. Since such systems cover a large-scale geographical area, synchronization to a global synchronized clock needs GPS based infrastructures which is not always convenient. In such circumstances, even though DGs have similar fixed sampling period times, they may start to sample their states at different time instants, resulting in asynchronous communication throughout the process. In the particular case of event-triggered controller design, the system's asynchronous communication behavior leads to asynchronous event-checking time instants. Therefore, we aim to design an event-triggered control mechanism that, beside its capability of reducing communication and computational complexity, is also able to handle asynchronous communication within the network. Accordingly, as illustrated in Fig. 2, despite of DGs' fixed periodic event-checking samplings, each of them may have different event-checking instants with respect to the rest of the microgrid system.

Let the common event-checking period be denoted by h and DGs' starting times $t_0^1, t_0^2, ..., t_0^N$ belong to the time interval $[0, h)$. Thus, each DG i checks its triggering condition at discrete times $t_0^i, t_1^i, \ldots$, where $t_k^i = t_0^i + kh$, $\forall k > 0$. Let the sequence $\left(t_{(0)}^i, t_{(1)}^i, \ldots\right)$ denotes the event instants of DG i, which is a subsequence of event-checking instants $\left(t_0^i, t_1^i, \ldots\right)$. Then, for $k = 0, 1, 2, \ldots$

$$\begin{cases} \hat{\omega}_i(t) = \omega_i(t_{(k)}^i), t_{(k)}^i \leq\ t < t_{(k+1)}^i \\ \hat{v}_{o,\mathrm{mag}i}(t) = v_{o,\mathrm{mag}i}(t_{(k)}^i), t_{(k)}^i \leq\ t < t_{(k+1)}^i \end{cases} \tag{7}$$

defines the latest broadcast operating frequency and output voltage of DG i at any given time t. In other words, $\hat{\omega}_i$ and $\hat{v}_{o,\mathrm{mag}i}$ are piecewise constant functions that only change value at event times.

B. Control Design

Given the assumptions and initialization described above, we investigate the frequency and voltage restoration problem for the asynchronous distributed system in (6) under periodic event-triggered control. The auxiliary control inputs are given as

$$\begin{cases} u_{\omega_i}(t) = -c_\omega e_{\omega_i}(t),\ t \geq h \\ u_{v_i}(t) = -c_v e_{v_i}(t),\ t \geq h \end{cases}, \tag{8}$$

where c_ω and $c_v \in R$ are the frequency and voltage control gains which adjust the convergence speed and $e_{\omega i}$ and e_{vi} are the following neighborhood tracking errors:

$$\begin{cases} e_{\omega_i}(t) = \sum_{j\in N_i} \tilde{a}_{ij}(\hat{\omega}_i(t) - \hat{\omega}_j(t)) \\ \qquad\qquad + \tilde{g}_i(\hat{\omega}_i(t) - \omega_{\mathrm{ref}}),\ t \geq h, \\ e_{v_i}(t) = \sum_{j\in N_i} \tilde{a}_{ij}(\hat{v}_{o,\mathrm{mag}i}(t) - \hat{v}_{o,\mathrm{mag}j}(t)) \\ \qquad\qquad + \tilde{g}_i(\hat{v}_{o,\mathrm{mag}i}(t) - v_{\mathrm{ref}}),\ t \geq h, \end{cases} \tag{9}$$

in which $\tilde{a}_{ij} \geq 0$ is the edge weight of the communication graph and indicates the communication strength between two connected DG i and DG j. The pinning gain denoted as $\tilde{g}_i$; $\tilde{g}_i > 0$ if and only if the DG i has access to the reference frequency and voltage information. For the secondary frequency controller, the time invariant and constant state of the leader (reference) node is denoted as ω_{ref}. For the secondary voltage controller, the state of the leader node is defined as v_{ref}. If v_{ref} is set to the nominal voltage of microgrid v_{nom}, the output voltage magnitude of DGs restore to this nominal voltage value. Meanwhile, v_{ref} can be chosen such that the output voltage magnitude of a critical bus of microgrid restores to microgrid nominal voltage v_{nom} [26]. A critical bus hosts the critical loads which are required to operate at the microgrid nominal voltage. Accordingly, v_{ref} is calculated as

$$v_{\mathrm{ref}} = k_p(v_{\mathrm{nom}} - v_{c,\mathrm{mag}}) + k_i \int (v_{\mathrm{nom}} - v_{c,\mathrm{mag}})dt, \tag{10}$$

where $v_{c,mag}$ is the voltage magnitude of the critical bus, and k_p and k_i are the proportional and integral PI controller parameters.

Due to the similarity between the frequency and voltage dynamical equations in (6), one can write these dynamics in the general form of

$$\dot{x}_i(t) = u_i(t), \tag{11}$$

where x_i denotes the DG specific dynamic and u_i is the auxiliary control input. Now, we recall and rewrite the auxiliary control inputs in (8) as

$$u_i(t) = -ce_i(t),\ t \geq h, \tag{12}$$

where,

$$e_i(t) = \sum_{j\in N_i} \tilde{a}_{ij}(\hat{x}_i(t) - \hat{x}_j(t)) + \tilde{g}_{ij}(\hat{x}_i(t) - \hat{x}_{\mathrm{ref}}(t)), \tag{13}$$

in which x_i represents either operating frequency or output voltage states of DG i. The state of the leader node is defined by x_{ref}. Also, c represents each of the frequency or voltage control gains.

From (13), the global tracking error vector can be defined as

$$e(t) = (\tilde{L} + \tilde{G})(\hat{x}(t) - x_{\text{ref}}\mathbf{1}_n),\ t \geq h, \tag{14}$$

where,

$$e(t) = [e_1(t), e_2(t), \ldots, e_n(t)]^T, \tag{15}$$

$$\hat{x}(t) = [\hat{x}_1(t), \hat{x}_2(t), \ldots, \hat{x}_n(t)]^T, \tag{16}$$

and $\mathbf{1}_n$ is the vector of all ones with size n. Let $\tilde{L}$ be the graph Laplacian of $\mathcal{G} = (V, E, A)$ and $\tilde{G} = \text{diag}(\tilde{g}_1, \tilde{g}_2, \ldots, \tilde{g}_n)$ be the pining gain vector.

Remark 1. In (12), updating control protocol u_i depends on the neighborhood tracking error e_i, which itself depends on the latest updated information of the piecewise constant functions $\hat{x}(t)$. Therefore, u_i is updated at both its own event times and those of its neighbors. Furthermore, it is worth mentioning that since the overall system does not synchronously start to activate and broadcast data, we assume for each DG i that $\tilde{a}_{ij} = 0$, $\forall t < \max\left(t_0^i, t_0^j\right)$.

Combining the controller gain c with the term $\tilde{L} + \tilde{G}$ and defining $\hat{\delta}(t) = (\hat{x}(t) - x_{\text{ref}}\mathbf{1}_n)$ as the global disagreement vector, given the global tracking error defined in (14), the closed-loop model for the linear system (6) is represented by

$$\dot{x}(t) = -(L + G)\hat{\delta}(t),\ t \geq\ h. \tag{17}$$

Motivated by the findings of [27], we suggest the following event-triggered condition:

$$|x_i(t_{(k)}^i + ph) - x_i(t_{(k)}^i)| > \sigma\sqrt{\frac{\int_{t_{(k)}^i+(p-1)h}^{t_{(k)}^i+ph}(L_i\hat{x}(s) + g_i(\hat{x}_i(s) - x_{\text{ref}}))^2\, ds}{h}}, \tag{18}$$

where σ is a positive scalar, L_i is the i^{th} row of the graph Laplacian L, and $t_{(k)}^i + ph$ is the p^{th} event-checking instant after the latest event at $t_{(k)}^i$ for DG i. It should be clear that decreasing σ enhances the chance of event occurring for each DG i at any given time.

Remark 2. The main purpose of the control mechanism based on the event condition (18) is to reduce the communication cost and the number of control updates while guaranteeing restoration for the operating frequency and output voltage magnitude of the system. Once the triggering condition is met, the current state of DG i is sampled and broadcast to its own controller as well as its neighbors. It should be noted that we do not consider time delays in communications in this work.

Before stating our main theorem, we define

$$\lambda = \max_{\|x\|_2=1} \frac{x^T(L+G)^T W(L+G)x}{x^T W(L+G)x}, \tag{19}$$

where $(L+G)^T W(L+G)$ and $W(L+G) + (L+G)^T W$ are positive-definite matrices. Moreover, denoting $A = L + G$ and recalling that $\hat{\delta}(t) = (\hat{x}(t) - x_{\text{ref}}\mathbf{1}_n)$ and $\delta(t) = (x(t) - x_{\text{ref}}\mathbf{1}_n)$, we have

$$\dot{\delta}(t) = -A\hat{\delta}(t). \tag{20}$$

We now state a sufficient condition under which the proposed control law leads to the convergence to consensus of all DGs' frequencies and output voltage magnitudes.

Theorem 1. *Given a strongly connected directed graph among the DGs, let the asynchronous system* (17) *be driven by the event-triggering mechanism* (18)*. Then, the operating frequency and output voltage magnitudes in terms of x_i, $1 \leq i \leq n$, converge to x_{ref} if the event checking period h and the positive parameter σ satisfy the inequality*

$$\frac{h}{2} + \sigma < \frac{1}{\lambda}. \tag{21}$$

The proof of Theorem 1 is provided in the Appendix. According to (6), ω_{ni} and V_{ni} are written as

$$\begin{cases} \omega_{ni} = \int (u_{\omega_i} + m_{Pi}\dot{P}_i)\, dt \\ V_{ni} = \int (u_{v_i} + n_{Qi}\dot{Q}_i)\, dt \end{cases}, \tag{22}$$

Although the secondary frequency and voltage controllers eliminate frequency and voltage steady-state deviations, they may lead to worse active and reactive power sharing compared to the primary controller. However, one expects that once the secondary control is applied, the control system will still be able to provide the same power sharing pattern guaranteed by the primary controller [6]. Applying the primary droop controller, the following equalities are then satisfied:

$$\begin{cases} m_{P_1}P_1 = \cdots = m_{P_n}P_n \\ n_{Q_1}Q_1 = \cdots = n_{Q_n}Q_n \end{cases}, \tag{23}$$

where m_{P_i} and n_{Q_i} denote the active and reactive power ratings of each DG i.

Similar to the primary controller, the secondary frequency and voltage controllers should guarantee (23). In order to achieve this requirement, an extra control input should be defined. Differentiating (23) and defining a control input, the power sharing problem is transformed to the consensus problem of first-order multi-agent systems

$$\begin{cases} m_{P_1}\dot{P}_1 = u_{P_1} \\ m_{P_2}\dot{P}_1 = u_{P_2} \\ \quad\vdots \\ m_{P_N}\dot{P}_1 = u_{P_N} \end{cases}, \begin{cases} n_{Q_1}\dot{Q}_1 = u_{Q_1} \\ n_{Q_2}\dot{Q}_1 = u_{Q_2} \\ \quad\vdots \\ n_{Q_N}\dot{Q}_1 = u_{Q_N} \end{cases}. \tag{24}$$

Given a strongly connected communication network topology among DGs, the auxiliary control inputs u_{Pi} and u_{Qi} are established as

$$\begin{cases} u_{P_i}(t) = -c_P e_{P_i}(t) \\ u_{Q_i}(t) = -c_Q e_{Q_i}(t) \end{cases}, \tag{25}$$

where c_P and c_Q are the active and reactive power control gains and e_{Pi} and e_{Qi} are the following neighboring tracking problems:

$$\begin{cases} e_{P_i}(t) = \sum_{j\in N_i} \tilde{a}_{ij}(m_{P_i}\hat{P}_i(t) - m_{P_j}\hat{P}_j(t)),\ t \geq h \\ e_{Q_i}(t) = \sum_{j\in N_i} \tilde{a}_{ij}(n_{Q_i}\hat{Q}_i(t) - n_{Q_j}\hat{Q}_j(t)),\ t \geq h \end{cases}, \tag{26}$$

This article has been accepted for publication in a future issue of this journal, but has not been fully edited. Content may change prior to final publication. Citation information: DOI 10.1109/TPWRS.2021.3059158, IEEE Transactions on Power Systems

Since the power sharing problem is a consensus problem, DGs must reach a non-prescribed agreement according to their power ratings. So compared to (9), there is no external reference input in (26). We now present the following event-triggering mechanisms

$$\begin{cases} |m_{Pi}P_i(t^i_{(k)}+ph) - m_{Pi}P_i(t^i_{(k)})| \\ > \sigma_P \sqrt{\frac{\int_{t^i_{(k)}+(p-1)h}^{t^i_{(k)}+ph} (\hat{\Omega}(s))^2\, ds}{h}}, \\ |n_{Qi}Q_i(t^i_{(k)}+ph) - n_{Qi}Q_i(t^i_{(k)})| \\ > \sigma_Q \sqrt{\frac{\int_{t^i_{(k)}+(p-1)h}^{t^i_{(k)}+ph} (\hat{\Psi}(s))^2\, ds}{h}}, \end{cases} \tag{27}$$

where

$$\begin{cases} \hat{\Omega}(s) = \sum_{j\in N} a_{ij}(m_{Pi}\hat{P}_i(s) - m_{Pj}\hat{P}_j(s)) \\ \hat{\Psi}(s) = \sum_{j\in N} a_{ij}(n_{Qi}\hat{Q}_i(s) - n_{Qj}\hat{Q}_j(s)) \end{cases}. \tag{28}$$

Using the same procedure as in Theorem 1, we can prove that the DGs active and reactive powers asymptotically converge to a common non-prescribed value. Then, the control input ω_{ni} and V_{ni} are written as

$$\begin{cases} \omega_{ni} = \int (u_{\omega_i} + u_{Pi})dt \\ V_{ni} = \int (u_{v_i} + u_{Qi})dt \end{cases}. \tag{29}$$

Fig. 3 illustrates the block diagram of the proposed secondary frequency and voltage controllers.

Remark 3. From practical standpoint, one should consider the effect of λ and its restrictions on the size of processors sampling periods as well as the number of events. The term λ itself is directly dependent on the controller gain c_ω, since we multiplied the graph Laplacian matrix by the controller gain c_w along the proof. Hence, determining appropriate λ is a trade-off problem between the speed of convergence and the computational complexity.

Algorithm 1 The proposed event-triggered distributed secondary control Algorithm.

Step 1 Initialize $p = 0$, $k = 0$, $t^i_{(0)} = t^i_0$

Step 2 Sample and store $x_i(t^i_{(0)}) = x_i(t^i_0)$ and send it to neighbors

Step 3 Loop:

- Check the event-triggering mechanisms, (18) and (27)

If both event-triggering conditions (18) and (27) hold,

-**then**:

- Update and broadcast $\hat{x}_i(t) = x_i(t^i_{(k)} + ph)$,
- $t^i_{(k)} = t^i_{(k)} + ph, k = k+1, p = 0$,
- **else**:
- broadcast the previous $\hat{x}_i(t)$ without updating
- $p = p + 1$.
- **end if**

NOTE: $x_i(t)$ represents each of the operating frequency, ω_i, output voltage magnitude, $v_{o,\mathrm{mag}i}$, active power, P_i and reactive power, Q_i of DG i.

TABLE I: Specification of the microgrid system.

DGs					
	DG 1 and 2			DG 3 and 4	
mP	9.4×10^{-5}			12.5×10^{-5}	
nQ	1.3×10^{-3}			1.4×10^{-3}	
Rc	0.03 Ω			0.03 Ω	
lC	0.35 mH			0.35 mH	
Rf	0.1 Ω			0.1 Ω	
Lf	1.35 mH			1.35 mH	
Cf	0.050 mF			0.050 mF	
KPV	0.1			0.05	
KIV	420			390	
KPC	15			10.5	
KIC	20000			16000	
Lines					
Line 1		Line 2		Line 3	
$Rl1$	0.23 Ω	$Rl2$	0.35 Ω	$Rl3$	0.23 Ω
$Ll1$	0.318 mH	$Ll2$	1.847 mH	$Ll3$	0.318 mH

V. Simulation and Experimental Verification

In this section, an islanded ac microgrid test system is developed in both simulation and experiment environments to demonstrate the performance of the proposed event-based frequency and voltage controllers through evaluating four case studies. In the first case, the proposed secondary control's ability to restore frequency and voltage deviations caused by droop controllers and accurate active and reactive power sharing is checked. Robustness of the proposed control scheme against model parameter uncertainty and load changes is evaluated in the second case. In the third case, the proposed asynchronous event-trigger-based method is separately compared against a conventional time-triggered method and a synchronous event-triggered algorithm. In the last case, the performance of the proposed method in the presence communication time delay is evaluated. Here, we consider a 380 V, 50 Hz microgrid system consisting of four DGs with a strongly connected communication graph $\mathcal{G}$ as shown in Fig. 4. The inner loop control parameters and load specifications are provided in Table I and II. Let the graph Laplacian of the communication topology be

$$\tilde{L} = \begin{bmatrix} 1 & 0 & 0 & -1 \\ -1 & 1 & 0 & 0 \\ 0 & -1 & 1 & 0 \\ 0 & 0 & -1 & 1 \end{bmatrix}. \tag{30}$$

TABLE II: Loads per phase of the microgrid system

Load 1		Load 2		Load 3		Load 4	
$R1$	10 Ω	$R2$	12.5 Ω	$R3$	5 Ω	$R4$	5 Ω
$L1$	0.035 H	$L2$	0.0175 H	$L3$	0.040 H	$L4$	0.040 H

DG 1 is the only DG that can access the reference with the pining gain of $\tilde{g} = 1$. The control gains c_ω, c_v, c_P, and c_Q are all set to 5. Then, multiplying the Laplacian graph by these gains, from (19), one can obtain $\lambda = 10$ for the graph Laplacian associated with the frequency and voltage controllers. Setting $\sigma_\omega = \sigma_P = 0.08$ and $\sigma_v = \sigma_Q = 0.01$, according to condition (21), all DGs are guaranteed to be restored if the sampling period is chosen sufficiently small to satisfy (21). We now pick a set of random time instants as $t^1_0 = 0$ s, $t^2_0 = 0.005$ s, $t^3_0 = 0.008$ s, $t^4_0 = 0.009$ s and set the event-checking period $h = 0.01$ s, which satisfies the condition

This article has been accepted for publication in a future issue of this journal, but has not been fully edited. Content may change prior to final publication. Citation information: DOI 10.1109/TPWRS.2021.3059158, IEEE Transactions on Power Systems

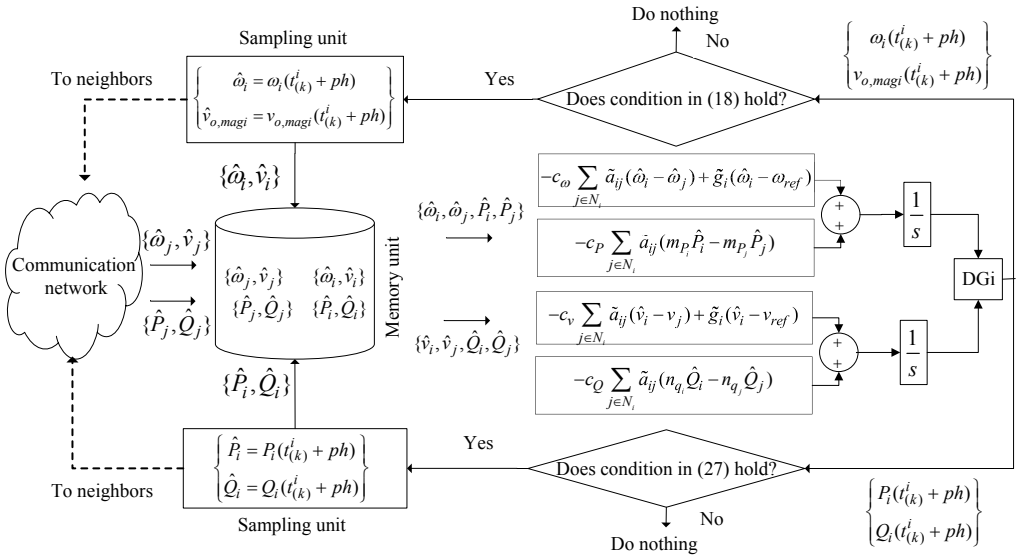

Fig. 3: Block diagram of the distributed secondary control with asynchronous periodic event-triggered communication mechanism.

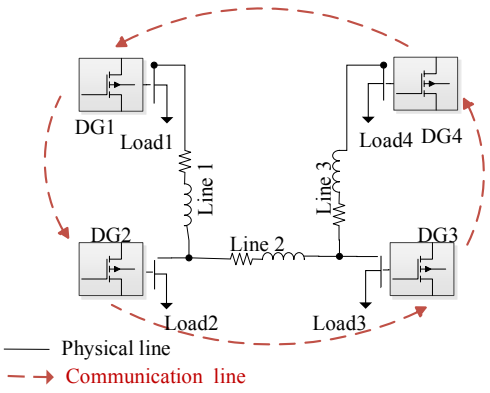

Fig. 4: Single-line diagram of the studies microgrid system.

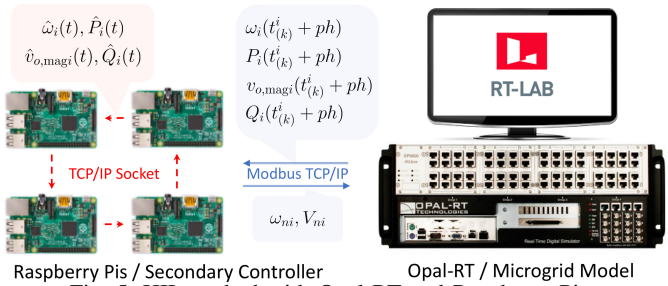

Fig. 5: HIL testbed with Opal-RT and Raspberry Pis.

(21). A detailed description of the proposed asynchronous periodic event-based secondary control scheme is presented in Algorithm 1.

The proposed asynchronous secondary controller is validated in the HIL testbed. The testbed is shown in Fig. 5. The 4-DG microgrid system shown in Fig. 4 is modeled in Simulink and runs in Opal-RT via RT-LAB. The secondary controllers of DGs are implemented in each Raspberry Pi. The communication is established through Modbus TCP/IP protocol. If the event-triggering conditions for frequency, active power, voltage, and reactive power are satisfied, $\hat{\omega}_i(t)$, $\hat{P}_i(t)$, $\hat{v}_{o,\mathrm{mag}i}(t)$, $\hat{Q}_i(t)$ are updated and transferred to neighbors via TCP/IP socket, respectively. Controller i calculates ω_{ni}, V_{ni} according to (29), and sends them to DG i through Modbus TCP/IP.

A. Case 1:Frequency and Voltage Restoration in Microgrid

In this subsection, we evaluate the ability of our proposed control method in frequency and voltage restoration. The microgrid is assumed to be islanded from the upstream grid at $t = 0$ and only the primary controller is activated.

Case 1.1 (Simulation Verification): As seen in Fig. 6(a) and Fig. 7(a) after islanding the microgrid, frequency and voltage terms of the DGs deviate from their reference values. The reference frequency ω_{ref} is set to 50 Hz. However, the aim of the voltage control is to restore the voltage of the critical bus. Therefore, v_{ref} is calculated using (10) with $k_p = 2$, $k_i = 1$, and $v_{\mathrm{nom}} = 380$ V. We herein assume that, DG4 hosts the critical loads. At $t = 2$ s, the secondary frequency and voltage controllers are activated. Fig. 6(a) shows that after applying the secondary controller, the dropped frequency terms of DGs are properly restored to their nominal values. Fig. 6(b) demonstrates that the control scheme applied restores frequency while sharing active power accurately. Fig. 7(a) shows that the voltage control scheme effectively returns the critical bus voltage amplitude to 380 V. Fig. 7(b) shows reactive power multiplied by reactive power droop coefficients of DGs. As seen, the proposed secondary voltage control scheme properly satisfies the same reactive power sharing pattern guaranteed by the primary controller.

Case 1.2 (Experimental Verification): To further investigate the proposed asynchronous event-triggered control strategy, HIL

This article has been accepted for publication in a future issue of this journal, but has not been fully edited. Content may change prior to final publication. Citation information: DOI 10.1109/TPWRS.2021.3059158, IEEE Transactions on Power Systems

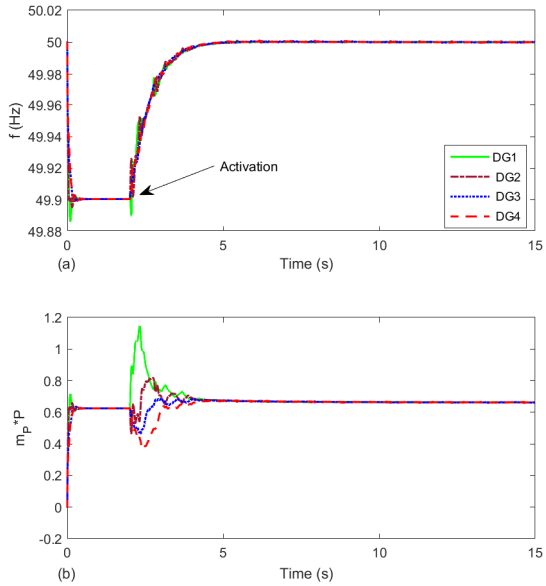

Fig. 6: Secondary frequency control in Case 1.1 (a) operating frequencies; (b) active power ratios.

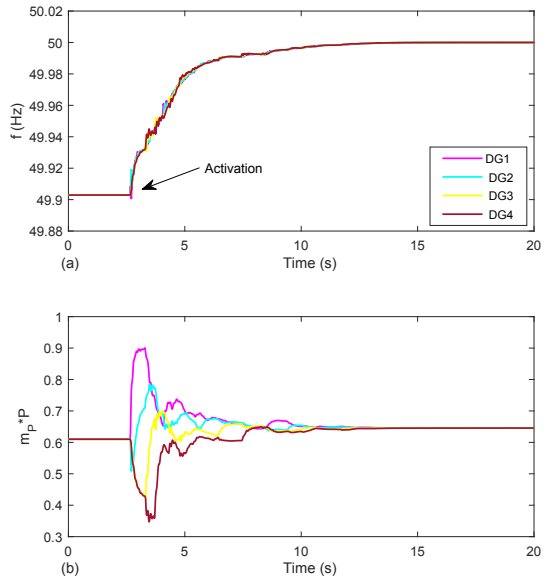

Fig. 8: Secondary frequency control in Case 1.2 (a) operating frequencies; (b) active power ratios.

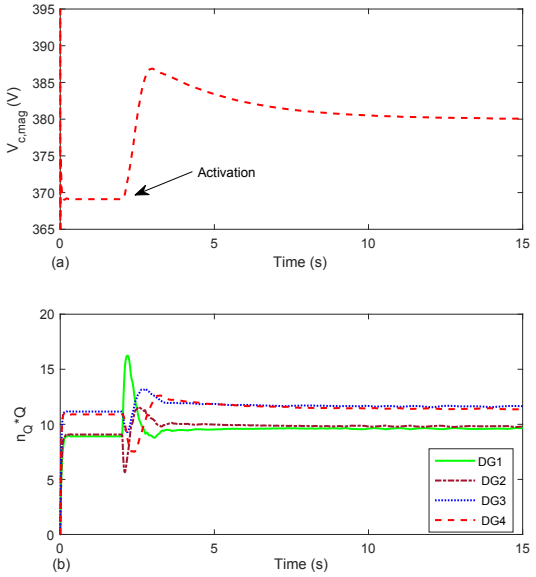

Fig. 7: Secondary voltage control in Case 1.1: (a) critical bus voltage; (b) reactive power ratios.

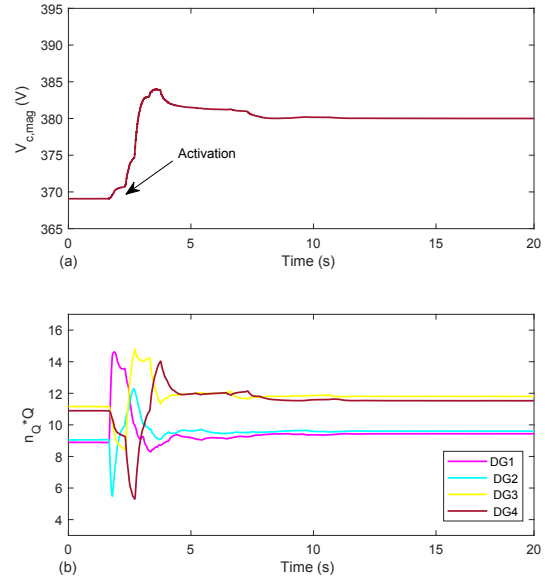

Fig. 9: Secondary voltage control in Case 1.2: (a) critical bus voltage; (b) reactive power ratios.

test is carried out to verify the effectiveness of the proposed algorithm. Similar to the simulation verification, we assume that in the first two seconds only the primary controller is activated. At $t = 2$ s, the secondary control loop is activated. Fig. 8 and Fig. 9 show the HIL experimental test results. These results demonstrate that the proposed mechanism effectively performs voltage and frequency restoration as well as active and reactive power sharing. Also, by comparing the simulation and experimental verification results, it is observed that the simulation and experimental test results match.

B. Case 2 Performance Analysis Against Model Parameter Uncertainty and Load Changes

In this subsection, robust performance of the proposed controller against model parameter uncertainty and load changes is tested. The simulation and experimental tests are carried out assuming 20% of additive DG's parameter uncertainty from their nominal values in Table I.

Case 2.1 (Simulation Verification): It is assumed that the microgrid system is disconnected from the main grid at $t = 2$ s and only the primary controller acts during the first two

This article has been accepted for publication in a future issue of this journal, but has not been fully edited. Content may change prior to final publication. Citation information: DOI 10.1109/TPWRS.2021.3059158, IEEE Transactions on Power Systems

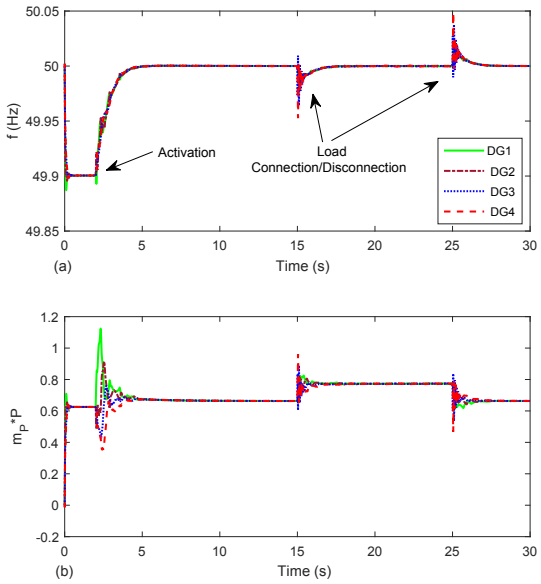

Fig. 10: Impact of parameter uncertainty and load changes in Case 2.1: (a) operating frequencies; (b) active power ratios.

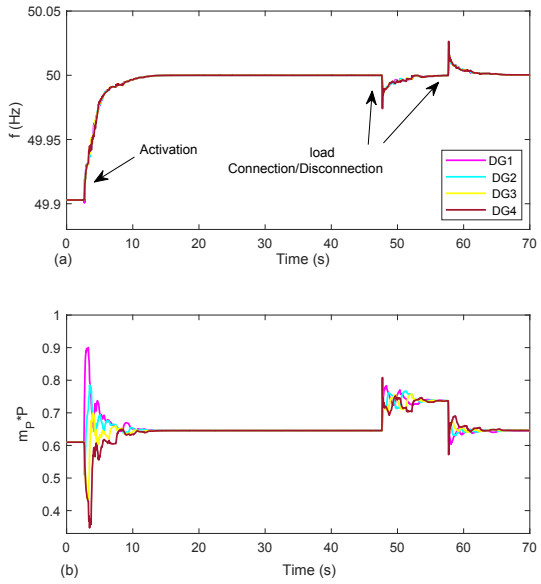

Fig. 12: Impact of parameter uncertainty and load changes in Case 2.2: (a) operating frequencies; (b) active power ratios.

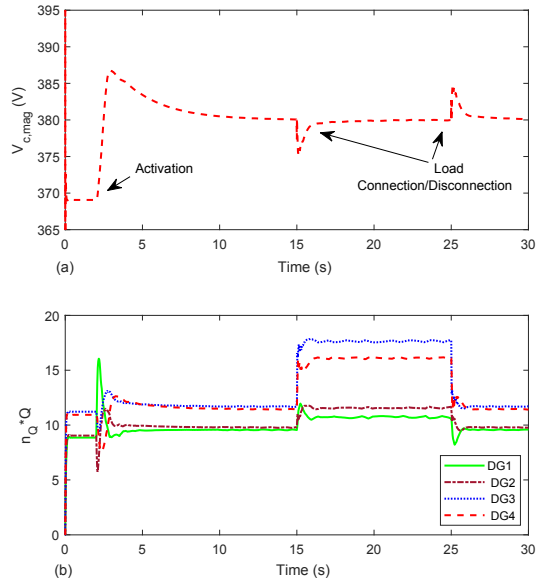

Fig. 11: Impact of parameter uncertainty and load changes in Case 2.1: (a) critical bus voltage; (b) reactive power ratios.

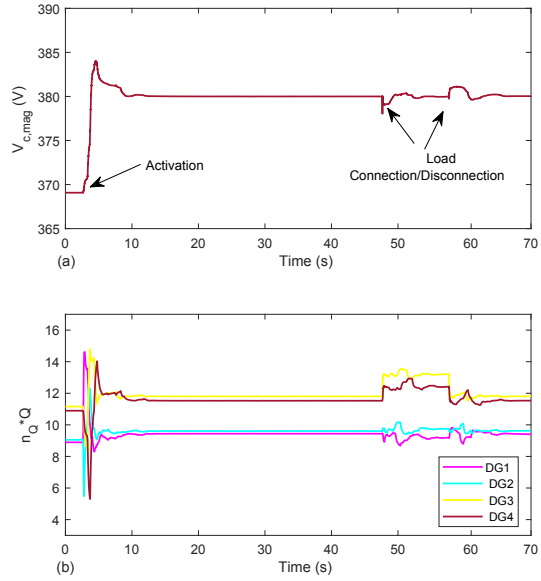

Fig. 13: Impact of parameter uncertainty and load changes in Case 2.2: (a) critical bus voltage; (b) reactive power ratios.

seconds. At $t = 2$ s, the secondary controller is activated, and then, a load change scenario is imposed at $t = 15$ s by connecting an RL load with $R = 5\ \Omega$ and $L = 40$ mH in parallel to load 3. To highlight the proposed control method's robust performance, we disconnect the added load at $t = 25$ s. Fig. 10(a) and Fig. 11(a) show that the proposed secondary control method is able to remarkably handle these load deviations and maintain frequency and voltage magnitudes at their nominal values. Fig. 10(b) depicts the capability of the secondary controller in guaranteeing accurate power sharing. As seen in Fig. 11(b), even in the presence of model parameter uncertainty and load changes the proposed secondary voltage control scheme is still able to properly satisfy reactive power sharing pattern.

Case 2.2 (Experimental Verification): It is assumed that the islanded microgrid experiences a load change at $t = 47$ s. To this end, an RL load with $R = 5\ \Omega$ and $L = 40$ mH is connected in parallel to load 3. The added load is then disconnected at $t = 57$ s. Fig. 12 and Fig. 13 show the HIL experimental test results. These results show that the proposed secondary control method is remarkably able to handle these load deviations in real environment and maintain

This article has been accepted for publication in a future issue of this journal, but has not been fully edited. Content may change prior to final publication. Citation information: DOI 10.1109/TPWRS.2021.3059158, IEEE Transactions on Power Systems

frequency and voltage magnitudes at their nominal rates while guaranteeing accurate power sharing.

C. Case 3: Comparison of the Proposed Asynchronous Event-triggered Secondary Control Against Conventional Synchronous Time-triggered and Event-triggered Techniques

In this subsection, the proposed asynchronous event-triggered microgrid control algorithm is first compared against the time-triggered algorithm in [6]. Then, the proposed algorithm is compared with the synchronous event-triggered algorithm in [28]. To this aim, we re-simulate Case 2 for both of the proposed methods in [6], [28]. It is assumed that $c_\omega = c_v = c_P = c_Q = 5$ and $\tilde{a}_{ij} = 1$ for all protocols. It should be noted that we have considered $\alpha = \beta = 0.45$ for the proposed event-triggered mechanism in [28]. Fig. 14 and Fig. 15 show the performance comparison between our proposed event-triggered method with the proposed methods in [6], [28]. To simplify the results, we only show the response of DG 4. The outcome underlines that in spite of asynchronous communication, which we considered in our case, the proposed control scheme has an identical performance in comparison with the proposed methods in [6] and [28], in terms of frequency and voltage restoration and active and reactive power sharing.

Focusing on the number of events during the eighteen-second simulation period wherein the secondary controller is activated, i.e., from $t = 2$ s to $t = 20$ s, the communication rates under our proposed method and the proposed methods in [6] and [28] are compared in Fig. 16. As seen in Fig. 16, the communication burden created by the proposed algorithm is lower than the other two algorithms. These results indicate that the proposed asynchronous periodic event-triggering algorithm effectively reduces the number of data transfers on the communication links.

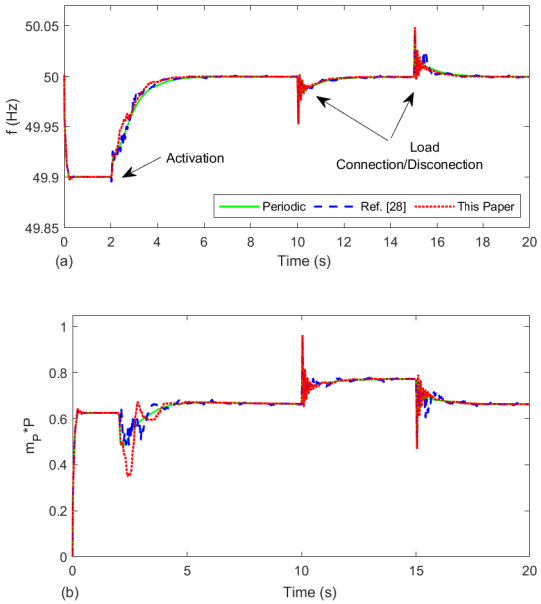

Fig. 14: Case 3: Performance comparison of the proposed frequency control method and the conventional ones presented in [6], [28].

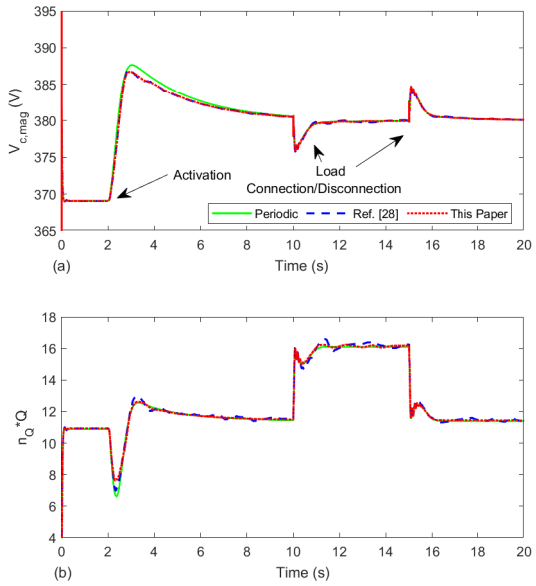

Fig. 15: Case 3: Performance comparison of the proposed voltage control method and the conventional ones presented in [6], [28].

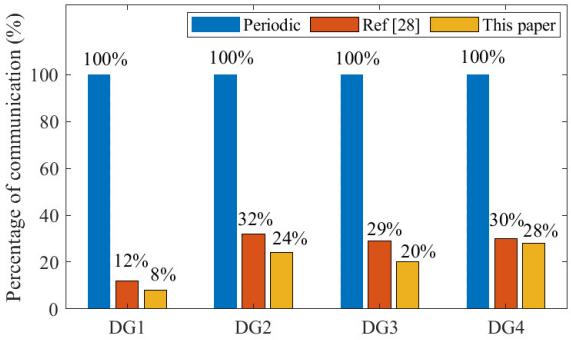

Fig. 16: Communication rate under different data exchange strategies

D. Case 4: Performance Evaluation In the Presence of Communication Time Delay

This study deals with evaluating the proposed control algorithm's performance in the presence of communication time delay. Similar to the previous case studies, it is assumed that the microgrid system is disconnected from the main grid at $t = 0$ s and only the primary controller acts in the first two seconds. At $t = 2$ s, the secondary frequency and voltage controllers are activated. Here, the communication time delay is assumed to be 120 ms. From Fig. 17 and Fig. 18, it is observed that frequency and voltage are successfully restored in the presence of time delay. It should also be emphasized that the communication delays are usually considered in the order of milliseconds or tens of milliseconds [16].

VI. Discussion

Convergence properties of linear consensus for distributed secondary control of microgrids have been increasingly developed in the literature since last decade. Many research works have been conducted to address a large set of problems in terms of consensus or in particular case event-triggered

This article has been accepted for publication in a future issue of this journal, but has not been fully edited. Content may change prior to final publication. Citation information: DOI 10.1109/TPWRS.2021.3059158, IEEE Transactions on Power Systems

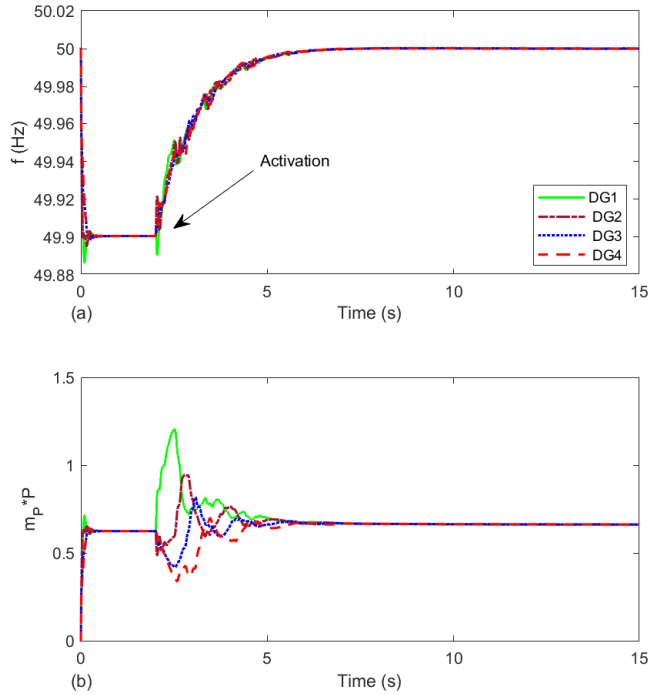

Fig. 17: Impact of communication time delay in Case 4: (a) DGs' operating frequencies; (b) active power ratios.

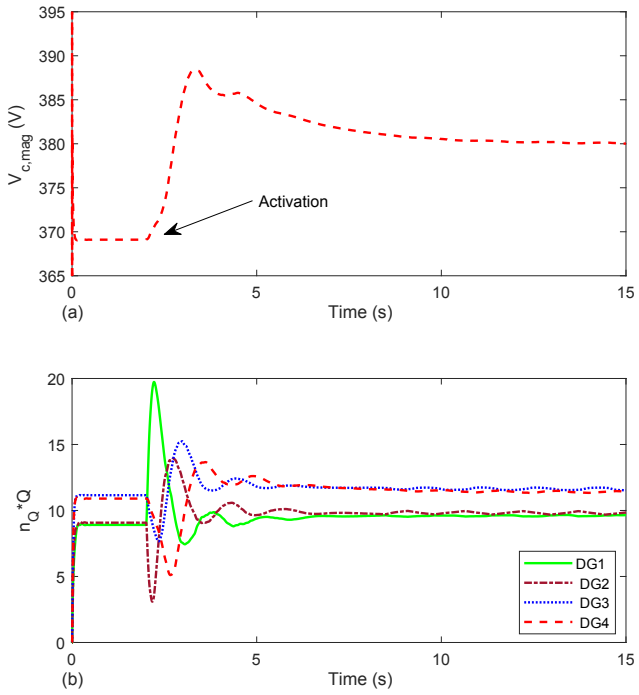

Fig. 18: Impact of communication time delay in Case 4: (a) critical bus voltage; (b) reactive power ratios.

consensus of microgrids. In the existing event-triggered microgrid distributed control techniques, it is assumed that all DGs are equipped with GPS clocks and communicate with each other in a synchronous manner. However, the GPS clocks may not be readily available or if existing, they may be exposed to cyber-attacks which render their operation ineffective. Accordingly, in this paper, a method is proposed to deal with such a situation in which DGs are not equipped with a common global clock and consequently receive asynchronous measurements from their neighboring DGs. Compared with traditional (time-/event-triggered) synchronous communication-based mechanisms, the proposed periodic event-triggered mechanism shows some prominent ability in reducing the communication rate among neighbors while guaranteeing stability and desired performance under asynchronous behavior of communication network. The proposed technique has been tested against different scenarios to verify its performance against microgrid islanding, load change, parameter uncertainty, and communication links' time delay. Moreover, the distributed secondary frequency and voltage control techniques are experimentally verified using a HIL testbed.

VII. Conclusion

In this paper, we have developed a distributed secondary frequency and voltage control scheme for an islanded ac microgrid in the case where DGs' clocks are not synchronized. In order to reduce communication and processors computational burden, a sampled-based event-triggered communication mechanism has been developed. In this mechanism, each DG checks its triggering condition periodically according to its own clock, which is possibly asynchronous to those of others. The proposed control scheme eliminates the need for a globally synchronized clock, making it more realistic and practical compared to existing methods. Developing a Lyapunov function, we have obtained a sufficient condition under which the proposed control laws steer DGs' frequencies and output voltage magnitudes to converge to the desired values. Finally, the effectiveness of the proposed method has been verified through simulating a microgrid test system under different scenarios in MATLAB/Simulink software environment and HIL platform.

In future work, we will move a step further to design controllers with triggering mechanisms that guarantee the asynchronous restoration problem for microgrid systems in which DGs have different sampling periods.

VIII. Appendix

This section is dedicated to the proof of Theorem 1. We consider the following candidate Lyapunov function,

$$V(t) = \frac{1}{2}\delta(t)^T W \delta(t). \tag{31}$$

From (20), differentiating $V(t)$ results in

$$\dot{V}(t) = -\delta(t)^T W A \hat{\delta}(t). \tag{32}$$

Let us now form a set comprising all DGs' controllers' event-checking instants, that is

$$\{t_k^i \mid 1 \leq i \leq N,\ k \geq 1\}. \tag{33}$$

This article has been accepted for publication in a future issue of this journal, but has not been fully edited. Content may change prior to final publication. Citation information: DOI 10.1109/TPWRS.2021.3059158, IEEE Transactions on Power Systems

Sorting all the instants in this set in the ascending order, a time sequence $t_0, t_1, \dots$ is obtained, starting from $t_0 = \min\{t_1^1, t_1^2, \dots, t_1^N\}$. Then, we have

$$\begin{aligned} V(t_{k+1}) &= V(t_0) + \int_{t_0}^{t_{k+1}} \dot{V}(s)ds \\ &= V(t_0) - \int_{t_0}^{t_{k+1}} \delta(s)^T W A\hat{\delta}(s)ds \\ &= V(t_0) - \sum_{i=1}^{n} \int_{t_0}^{t_{k+1}} w_i \delta_i(s)^T A_i \hat{\delta}(s)ds. \end{aligned} \tag{34}$$

Recalling that h is the event-checking period for all DGs, it should be clear that, given any k, for each $i \in \{1, 2, \dots, N\}$, there exists a p_i such that $t_{p_i+1}^i < t_{k+1} \le t_{p_i+1}^i + h$. Therefore, one can write

$$\begin{aligned} &\int_{t_0}^{t_{k+1}} w_i \delta_i(s) A_i \hat{\delta}(s)ds \\ &= (\int_{t_0}^{t_1^i} + \int_{t_1^i}^{t_2^i} + \cdots + \int_{t_q^i}^{t_{q+1}^i} + \dots \\ &+ \int_{t_{p_i}^i}^{t_{p_i+1}^i} + \int_{t_{p_i+1}^i}^{t_{k+1}}) w_i \delta_i(s) A_i \hat{\delta}(s)ds. \end{aligned} \tag{35}$$

Given any q, if $t_r = t_q^i$, $t_{r+k'} \le t_{q+1}^i$, using (20), we have

$$\begin{aligned} &\int_{t_q^i}^{t_{r+k'}} w_i \delta_i(s) A_i \hat{\delta}(s)ds \\ &= \int_{t_q^i}^{t_{r+k'}} \left(\delta_i(t_q^i) - \int_{t_q^i}^{s} A_i \hat{\delta}(t)dt \right) w_i A_i \hat{\delta}(s)ds \\ &= \int_{t_q^i}^{t_{r+k'}} w_i \delta_i(t_q^i) A_i \hat{\delta}(s)ds \\ &- \int_{t_q^i}^{t_{r+k'}} \left(\int_{t_q^i}^{s} A_i \hat{\delta}(t)dt \right) w_i A_i \hat{\delta}(s)ds. \end{aligned} \tag{36}$$

We further calculate the last two terms in (36) as follows. First, we write

$$\begin{aligned} &\int_{t_q^i}^{t_{r+k'}} \left(\int_{t_q^i}^{s} A_i \hat{\delta}(t)dt \right) w_i A_i \hat{\delta}(s)ds \\ &= \frac{1}{2} w_i \left(\int_{t_q^i}^{t_{r+k'}} A_i \hat{\delta}(t)dt \right)^2 \\ &= \frac{1}{2} w_i \left(\int_{t_r}^{t_{r+1}} A_i \hat{\delta}(t)dt + \cdots + \int_{t_{r+k'-1}}^{t_{r+k'}} A_i \hat{\delta}(t)dt \right)^2 \\ &= \frac{1}{2} w_i ((t_{r+1} - t_r) A_i \hat{\delta}(t_r) + (t_{r+2} - t_{r+1}) A_i \hat{\delta}(t_{r+1}) \\ &+ \cdots + (t_{r+k'} - t_{r+k'-1}) A_i \hat{\delta}(t_{r+k'-1}))^2 \\ &= \frac{h^2}{2} w_i (\frac{t_{r+1} - t_r}{h} A_i \hat{\delta}(t_r) + \frac{t_{r+2} - t_{r+1}}{h} A_i \hat{\delta}(t_{r+1}) \\ &+ \cdots + \frac{t_{r+k'} - t_{r+k'-1}}{h} A_i \hat{\delta}(t_{r+k'-1}))^2 \\ &\le \frac{h^2}{2} w_i (\frac{t_{r+1} - t_r}{h} (A_i \hat{\delta}(t_r))^2 + \frac{t_{r+2} - t_{r+1}}{h} (A_i \hat{\delta}(t_{r+1}))^2 \\ &+ \cdots + \frac{t_{r+k'} - t_{r+k'-1}}{h} (A_i \hat{\delta}(t_{r+k'-1}))^2) \\ &= \frac{h}{2} \sum_{p=r}^{r+k'-1} (t_{p+1} - t_p) w_i \hat{\delta}(t_p)^T A_i^T A_i \hat{\delta}(t_p). \end{aligned} \tag{37}$$

Second, defining $\Delta_i(s) = \delta_i(t_q^i) - \hat{\delta}_i(t_q^i)$, $t_q^i \le s < t_{q+1}^i$, and $\Delta(s) = [\Delta_1(s)\Delta_2(s) \dots \Delta_n(s)]^T$, we write

$$\begin{aligned} &\int_{t_q^i}^{t_{r+k'}} w_i \delta_i(t_q^i) A_i \hat{\delta}(s)ds \\ &= \int_{t_q^i}^{t_{r+k'}} (\hat{\delta}_i(t_q^i) + \Delta_i(t_q^i)) w_i A_i \hat{\delta}(s)ds \\ &= \int_{t_q^i}^{t_{r+k'}} w_i \hat{\delta}_i(s) A_i \hat{\delta}_i(s)ds + \int_{t_q^i}^{t_{r+k'}} w_i \Delta_i(t_q^i) A_i \hat{\delta}(s)ds \\ &= \sum_{q=r}^{r+k'-1} \int_{t_q}^{t_{q+1}} w_i \hat{\delta}_i(s) A_i \hat{\delta}_i(s)ds \\ &+ \int_{t_q^i}^{t_{r+k'}} w_i \Delta_i(t_q^i) A_i \hat{\delta}(s)ds. \end{aligned} \tag{38}$$

Recalling the event-triggering condition (18), one notices that the following inequality holds for any q:

$$|\Delta_i(t_q^i)| = |\delta_i(t_q^i) - \hat{\delta}_i(t_q^i)| \le \sigma \sqrt{\frac{\int_{t_{q-1}^i}^{t_q^i} (A_i \hat{\delta}(s))^2 ds}{h}}, \quad i = 1, \dots, n. \tag{39}$$

More precisely, if an event occurs at t_q^i, then $\hat{\delta}_i(t_q^i) = \delta_i(t_q^i)$, which means that (39) holds. If no event occurs at t_q^i, then $\hat{\delta}_i(t_q^i) = \hat{\delta}_i(t_{q-1}^i)$, meaning that the event-triggering condition (18) is not satisfied, implying that (39) holds.

This article has been accepted for publication in a future issue of this journal, but has not been fully edited. Content may change prior to final publication. Citation information: DOI 10.1109/TPWRS.2021.3059158, IEEE Transactions on Power Systems

From (39), we conclude for the last term in (38) that

$$\begin{aligned}
&-\int_{t_q^i}^{t_{r+k'}} w_i\Delta_i(t_q^i)A_i\hat{\delta}(s)ds\\
&\le \int_{t_q^i}^{t_{r+k'}} w_i[\frac{1}{\sigma}(\Delta_i(t_q^i))^2+\sigma(A_i\hat{\delta}(s))^2]ds\\
&=\frac{1}{2\sigma}(t_{r+k'}-t_q^i)w_i(\Delta_i(t_q^i))^2+\frac{\sigma}{2}\int_{t_q^i}^{t_{r+k'}} w_i(A_i\hat{\delta}(s))^2ds\\
&\le \frac{1}{2\sigma}h\sigma^2\frac{\int_{t_{q-1}^i}^{t_q^i} w_i(A_i\hat{\delta}(s))^2ds}{h}+\frac{\sigma}{2}\int_{t_q^i}^{t_{r+k'}} w_i(A_i\hat{\delta}(s))^2ds\\
&=\frac{\sigma}{2}\int_{t_{q-1}^i}^{t_q^i} w_i\hat{\delta}(s)^TA_i^TA_i\hat{\delta}(s)ds\\
&+\frac{\sigma}{2}\int_{t_q^i}^{t_{r+k'}} w_i\hat{\delta}(s)^TA_i^TA_i\hat{\delta}(s)ds.
\end{aligned}\tag{40}$$

Therefore,

$$\begin{aligned}
&-(\int_{t_1^i}^{t_2^i} w_i\Delta_i(t_1^i)A_i\hat{\delta}(s)ds\\
&+\int_{t_2^i}^{t_3^i} w_i\Delta_i(t_2^i)A_i\hat{\delta}(s)ds+\dots\\
&+\int_{t_{p_i+1}}^{t_{k+1}} w_i\Delta_i(t_{p_i+1}^i)A_i\hat{\delta}(s)ds)\\
&\le \frac{\sigma}{2}\int_{t_0^i}^{t_1^i} w_i\hat{\delta}(s)^TA_i^TA_i\hat{\delta}(s)ds\\
&+\sigma\int_{t_1^i}^{t_{k+1}} w_i\hat{\delta}(s)^TA_i^TA_i\hat{x}sds.
\end{aligned}\tag{41}$$

Set $t_{k_0}=\max_{1\le i\le n}\{t_1^i\}$ and $t_{k_0^i}^i=t_1^i$, and denote

$$\begin{aligned}
V_0&=-\sum_{i=1}^n\int_{t_0}^{t_1^i} w_i\delta_iA_i\hat{\delta}(s)ds\\
&-\sum_{i=1}^n\sum_{p=k_0}^{k_0-1}\int_{t_p}^{t_{p+1}} w_i\hat{\delta}_i(s)L_i\hat{x}(s)ds\\
&+\frac{\sigma}{2}\sum_{i=1}^n\int_{t_0^i}^{t_1^i} w_i\hat{\delta}(s)A_i^TA_i\hat{\delta}(s)ds\\
&+(\frac{h}{2}+\sigma)\sum_{i=1}^n\sum_{p=k_0^i}^{k_0-1}(t_{p+1}-t_p)w_i\hat{\delta}(t_p)^TA_i^TA_i\hat{\delta}(t_p).
\end{aligned}\tag{42}$$

It follows from formulas (35)-(41) that

$$\begin{aligned}
V(t_{k+1})&=V(t_0)-\sum_{i=1}^n\int_{t_0}^{t_{k+1}} w_i\delta_i(s)A_i\hat{\delta}(s)ds\\
&=V(t_0)-\sum_{i=1}^n\int_{t_0}^{t_1^i} w_i\delta_i(s)A_i\hat{\delta}(s)ds\\
&-\sum_{i=1}^n\int_{t_1^i}^{t_{k+1}} w_i\delta_i(s)A_i\hat{\delta}(s)ds\\
&\le V(t_0)-\sum_{i=1}^n\int_{t_0}^{t_1^i} w_i\delta_i(s)A_i\hat{\delta}(s)ds\\
&-\sum_{i=1}^n\sum_{p=k_0^i}^{k}\int_{t_p}^{t_{p+1}} w_i\hat{\delta}_i(s)A_i\hat{\delta}(s)ds\\
&+\frac{\sigma}{2}\sum_{i=1}^n\int_{t_0^i}^{t_1^i} w_i\hat{\delta}(s)^TA_i^TA_i\hat{\delta}(s)ds\\
&+\sigma\sum_{i=1}^n\int_{t_1^i}^{t_{k+1}} w_i\hat{\delta}(s)^TA_i^TA_i\hat{\delta}(s)ds\\
&+\frac{h}{2}\sum_{i=1}^n\sum_{p=k_0^i}^{k}(t_{p+1}-t_p)w_i\hat{\delta}(t_p)^TA_i^TA_i\hat{\delta}(t_p)\\
&=V(t_0)+V_0
\end{aligned}\tag{43}$$

$$\begin{aligned}
&-\sum_{p=k_0}^{k}(t_{p+1}-t_p)w_i\hat{\delta}(t_p)^TWA\hat{\delta}(t_p)\\
&(\frac{h}{2}+\sigma)\sum_{p=k_0}^{k}(t_{p+1}-t_p)w_i\hat{\delta}(t_p)^TA^TWA\hat{\delta}(t_p)\\
&\le V(t_0)+V_0\\
&-(1-\lambda(\frac{h}{2}+\sigma))\sum_{p=k_0}^{k}(t_{p+1}-t_p)\hat{\delta}(t_p)^TWA\hat{\delta}(t_p).
\end{aligned}\tag{44}$$

Combination of (21) and the fact that $V(t)\ge 0$ results in

$$\lim_{k\to\infty}(t_{k+1}-t_k)\hat{\delta}(t_k)^TWA\hat{\delta}(t_k)=0.\tag{45}$$

Noticing that t_k and t_{k+1} are consecutive elements of the set defined by (33), $t_{k+1}-t_k$ is uniformly lower bounded by a fixed positive number. We thus conclude that

$$\lim_{k\to\infty}\hat{\delta}(t_k)^TWA\hat{\delta}(t_k)=0.\tag{46}$$

Then, recalling (19), we have

$$\hat{\delta}(t_k)^TA^TWA\hat{\delta}(t_k)\le\lambda\hat{\delta}(t_k)^TWA\hat{\delta}(t_k),\tag{47}$$

which immediately implies that $\lim_{k\to\infty}A\hat{\delta}(t_k)=0$. This, together with (7), result in

$$\lim_{t\to\infty}A\hat{\delta}(t)=0,\tag{48}$$

or equivalently,

$$\lim_{t\to\infty}\dot{\delta}(t)=0.\tag{49}$$

Relations (48) and (39) imply that for any i,

$$\lim_{k\to\infty}(\delta_i(t_k^i)-\hat{\delta}_i(t_k^i))=0.\tag{50}$$

Since for any t, there exists a positive integer k_t such that $t\in[t_{k_t}^i,t_{k_t+1}^i]$, we can write

$$\begin{aligned}
&\lim_{t\to\infty}(\delta_i(t)-\hat{\delta}_i(t))\\
&=\lim_{t\to\infty}(\delta_i(t)-\delta_i(t_{k_t}^i)+\delta_i(t_{k_t}^i)-\hat{\delta}_i(t))\\
&=\lim_{t\to\infty}\left(\int_{t_{k_t}^i}^{t}\dot{\delta}_i(s)ds+\delta_i(t_{k_t}^i)-\hat{\delta}_i(t_{k_t}^i)\right)=0.
\end{aligned}\tag{51}$$

We note that the last equality in (51) is deduced from (49) and (50). From (51), we conclude that $\lim_{t\to\infty}(\delta(t)-\hat{\delta}(t))=$

0, and consequently $\lim_{t\to\infty}(A\delta(t) - A\hat{\delta}(t)) = 0$. Thus, $\lim_{t\to\infty} A\delta(t) = 0$. Hence,

$$\begin{aligned}&\lim_{t\to\infty} \delta(t)^T W A\delta(t)\\ &= \lim_{t\to\infty} \delta(t)^T \left(\frac{WL + L^T W}{2} + WG\right)\delta(t) = 0,\end{aligned} \tag{52}$$

which leads to

$$\lim_{t\to\infty} \delta(t) = 0. \tag{53}$$

Thus, we finally arrive at

$$\lim_{t\to\infty} x(t) = \lim_{t\to\infty} (\delta(t) + x_{\text{ref}} 1_n) = x_{\text{ref}} \mathbf{1}_n, \tag{54}$$

which completes the proof. □

REFERENCES

[1] M. Farrokhabadi, C. A. Cañizares, J. W. Simpson-Porco, E. Nasr, L. Fan, P. A. Mendoza-Araya, R. Tonkoski, U. Tamrakar, N. Hatziargyriou, D. Lagos *et al.*, "Microgrid stability definitions, analysis, and examples," *IEEE Trans. Power Systems*, vol. 35, no. 1, pp. 13–29, 2019.

[2] R. H. Lasseter, "Microgrids," in *2002 IEEE Power Engineering Society Winter Meeting. Conference Proceedings (Cat. No. 02CH37309)*, vol. 1. IEEE, 2002, pp. 305–308.

[3] A. Bidram and A. Davoudi, "Hierarchical structure of microgrids control system," *IEEE Trans. Smart Grid*, vol. 3, no. 4, pp. 1963–1976, 2012.

[4] J. M. Guerrero, J. C. Vasquez, J. Matas, L. G. De Vicuña, and M. Castilla, "Hierarchical control of droop-controlled ac and dc microgrids—a general approach toward standardization," *IEEE Trans. industrial electronics*, vol. 58, no. 1, pp. 158–172, 2010.

[5] A. Mehrizi-Sani and R. Iravani, "Potential-function based control of a microgrid in islanded and grid-connected modes," *IEEE Trans. Power Systems*, vol. 25, no. 4, pp. 1883–1891, 2010.

[6] A. Bidram, A. Davoudi, F. L. Lewis, and Z. Qu, "Secondary control of microgrids based on distributed cooperative control of multi-agent systems," *IET Generation, Transmission & Distribution*, vol. 7, no. 8, pp. 822–831, 2013.

[7] J. Qin, Q. Ma, Y. Shi, and L. Wang, "Recent advances in consensus of multi-agent systems: A brief survey," *IEEE Trans. Industrial Electronics*, vol. 64, no. 6, pp. 4972–4983, 2016.

[8] Y. Cao, W. Yu, W. Ren, and G. Chen, "An overview of recent progress in the study of distributed multi-agent coordination," *IEEE Trans. Industrial informatics*, vol. 9, no. 1, pp. 427–438, 2012.

[9] M. M. Gulzar, S. T. H. Rizvi, M. Y. Javed, U. Munir, and H. Asif, "Multi-agent cooperative control consensus: A comparative review," *Electronics*, vol. 7, no. 2, p. 22, 2018.

[10] T. Henningsson, E. Johannesson, and A. Cervin, "Sporadic event-based control of first-order linear stochastic systems," *Automatica*, vol. 44, no. 11, pp. 2890–2895, 2008.

[11] J. Lunze and D. Lehmann, "A state-feedback approach to event-based control," *Automatica*, vol. 46, no. 1, pp. 211–215, 2010.

[12] Z. Zhang, S. Gong, A. D. Dimitrovski, and H. Li, "Time synchronization attack in smart grid: Impact and analysis," *IEEE Transactions on Smart Grid*, vol. 4, no. 1, pp. 87–98, 2013.

[13] A. Bidram, A. Davoudi, F. L. Lewis, and J. M. Guerrero, "Distributed cooperative secondary control of microgrids using feedback linearization," *IEEE Trans. Power Systems*, vol. 28, no. 3, pp. 3462–3470, 2013.

[14] Y. Xu, H. Sun, W. Gu, Y. Xu, and Z. Li, "Optimal distributed control for secondary frequency and voltage regulation in an islanded microgrid," *IEEE Trans. Industrial Informatics*, vol. 15, no. 1, pp. 225–235, 2018.

[15] M. A. Shahab, B. Mozafari, S. Soleymani, N. M. Dehkordi, H. M. Shourkaei, and J. M. Guerrero, "Stochastic consensus-based control od μs with communication delays and noises," *IEEE Trans. Power Systems*, vol. 34, no. 5, pp. 3573–3581, 2019.

[16] C. Ahumada, R. Cárdenas, D. Saez, and J. M. Guerrero, "Secondary control strategies for frequency restoration in islanded microgrids with consideration of communication delays," *IEEE Trans. Smart Grid*, vol. 7, no. 3, pp. 1430–1441, 2015.

[17] D. O. Amoateng, M. Al Hosani, M. S. Elmoursi, K. Turitsyn, and J. L. Kirtley, "Adaptive voltage and frequency control of islanded multi-microgrids," *IEEE Trans. Power Systems*, vol. 33, no. 4, pp. 4454–4465, 2017.

[18] L. Ding, Q.-L. Han, and X.-M. Zhang, "Distributed secondary control for active power sharing and frequency regulation in islanded microgrids using an event-triggered communication mechanism," *IEEE Trans. Industrial Informatics*, vol. 15, no. 7, pp. 3910–3922, 2018.

[19] D. Pullaguram, S. Mishra, and N. Senroy, "Event-triggered communication based distributed control scheme for dc microgrid," *IEEE Trans. Power Systems*, vol. 33, no. 5, pp. 5583–5593, 2018.

[20] Y. Fan, G. Hu, and M. Egerstedt, "Distributed reactive power sharing control for microgrids with event-triggered communication," *IEEE Trans. Control Systems Technology*, vol. 25, no. 1, pp. 118–128, 2016.

[21] J. Zhou, Y. Xu, H. Sun, L. Wang, and M.-Y. Chow, "Distributed event-triggered h_∞ consensus based current sharing control of dc microgrids considering uncertainties," *IEEE Trans. Industrial Informatics*, 2019.

[22] W. Ren, R. W. Beard, and E. M. Atkins, "Information consensus in multivehicle cooperative control," *IEEE Control systems magazine*, vol. 27, no. 2, pp. 71–82, 2007.

[23] F. Xiao, L. Wang, J. Chen, and Y. Gao, "Finite-time formation control for multi-agent systems," *Automatica*, vol. 45, no. 11, pp. 2605–2611, 2009.

[24] N. Pogaku, M. Prodanovic, and T. C. Green, "Modeling, analysis and testing of autonomous operation of an inverter-based microgrid," *IEEE Trans. power electronics*, vol. 22, no. 2, pp. 613–625, 2007.

[25] M. Rasheduzzaman, J. A. Mueller, and J. W. Kimball, "Reduced-order small-signal model of microgrid systems," *IEEE Trans. Sustainable Energy*, vol. 6, no. 4, pp. 1292–1305, 2015.

[26] A. Bidram, B. Poudel, L. Damodaran, R. Fierro, and J. M. Guerrero, "Resilient and cybersecure distributed control of inverter-based islanded microgrids," *IEEE Transactions on Industrial Informatics*, vol. 16, no. 6, pp. 3881–3894, 2019.

[27] A. Wang, B. Mu, and Y. Shi, "Consensus control for a multi-agent system with integral-type event-triggering condition and asynchronous periodic detection," *IEEE Trans. Industrial Electronics*, vol. 64, no. 7, pp. 5629–5639, 2017.

[28] M. Chen, X. Xiao, and J. M. Guerrero, "Secondary restoration control of islanded microgrids with a decentralized event-triggered strategy," *IEEE Trans. Industrial Informatics*, vol. 14, no. 9, pp. 3870–3880, 2017.

KEYWAN MOHAMMADI received his B.S. degree in Electrical Engineering from University of Kurdistan, Sanandaj, Iran in 2017, and obtained his M.S. in Control Engineering from Tarbiat Modares University (TMU), Tehran, Iran in 2020. Since 2020, he has been with the Department of Electrical and Computer Engineering, Tarbiat Modares University, as a Research Assistant. His research interests broadly include areas of Networked Control Systems, Machine Learning, Control of Microgrid Systems, and Autonomous Vehicles.

ELNAZ AZIZI (S'20) received the B.Sc. M.Sc. degrees in electrical engineering from the University of Tabriz, Tabriz, Iran in 2014, and 2016, respectively. She is a Ph.D. candidate in the Electrical and Computer Engineering Department at Tarbiat Modares University, Tehran, Iran, and a visiting research scholar at the Department of Electrical Power Engineering and Mechatronics at Tallinn University of Technology, Tallinn, Estonia. Her research interests include machine learning, smart grid, and optimization.

JEEWON CHOI (S'20) received the B.S. degree in mechanical and automotive engineering from Keimyung University, Daegu, South Korea, in 2015, and M.S. degree in mechanical engineering from the University of New Mexico, Albuquerque, NM, USA, in 2018, where she is currently pursuing the Ph.D. degree in mechanical engineering. Her research interests include smart grid, microgrid, and cyber-physical system modeling and simulation.

MOHAMMAD T.H. BEHESHTI (S'86-M'93) received his BS degree in Electrical Engineering from the University of Nebraska at Lincoln in 1984, and his MS and PhD degrees in Control Engineering from the Wichita State University, Kansas, in 1987 and 1992, respectively. Since 1995 he has been working as an associate professor of Electrical and Computer Engineering Department at Tarbiat Modares University, Tehran, Iran. His research interests include modelling and control of singular perturbation systems and modelling and control of communication and computer networks. Modeling and Control of Smart Grids and Microgrids.

ALI BIDRAM (S'12-M'17-SM'20) is currently an Assistant Professor in the Electrical and Computer Engineering Department, University of New Mexico, Albuquerque, NM, USA. He has received his B.Sc. and M.Sc. from Isfahan University of Technology, Iran, in 2008 and 2010, and Ph.D. from the University of Texas at Arlington, USA, in 2014. Before joining University of New Mexico, he worked with Quanta Technology, LLC, and was involved in a wide range of projects in electric power industry. He is an Associate Editor for the IEEE Transactions on Industry Applications.

His area of expertise lies within control and coordination of energy assets in power electronics-intensive energy distribution grids. Such research efforts are culminated in a book, several journal papers in top publication venues and articles in peer-reviewed conference proceedings, and technical reports. He has received IEEE Albuquerque section outstanding engineering educator award, New Mexico EPSCoR mentorship award, University of Texas at Arlington N. M. Stelmakh outstanding student research award, Quanta Technology Shooting Star award, IEEE Kansas Power and Energy Conference best paper award, and cover article of December 2014 in IEEE Control Systems.

SADEGH BOLOUKI (M'14) received the B.S. and Ph.D. degrees in Electrical Engineering from Sharif University of Technology, Tehran, Iran and Polytechnique Montréal, Montreal, QC, Canada in 2008 and 2014, respectively. Since September 2018, he has been an Assistant Professor of Electrical and Computer Engineering in Tarbiat Modares University, Tehran, Iran. He is also a Research Associate with the Department of Mechanical Engineering in Polytechnique Montréal, Montreal, Canada. His past experience includes postdoctoral tenures at the Department of Mechanical Engineering and Mechanics, Lehigh University, PA, USA and Coordinated Science Laboratory, University of Illinois at Urbana-Champaign, IL, USA. His research interests broadly include the areas of machine learning, network science, and game theory.